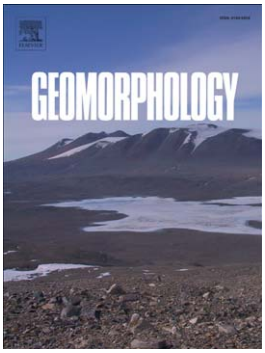

Planform and mobility in the meaípe-maimbá embayed beach on the South East coast of Brazil

Jacqueline Albino, José A. Jiménez, Tiago C.A. Oliveira

PII: S0169-555X(15)30158-6
DOI: doi: 10.1016/j.geomorph.2015.09.024
Reference: GEOMOR 5391

To appear in: *Geomorphology*

Received date: 17 November 2014
Revised date: 25 September 2015
Accepted date: 27 September 2015

Please cite this article as: Albino, Jacqueline, Jiménez, José A., Oliveira, Tiago C.A., Planform and mobility in the meaípe-maimbá embayed beach on the South East coast of Brazil, *Geomorphology* (2015), doi: 10.1016/j.geomorph.2015.09.024

Planform and mobility in the Meaípe-Maimbá embayed beach on the South East coast of Brazil

Jacqueline Albino*[1], José A. Jiménez[2] and Tiago C. A. Oliveira[3]

[1] Department of Oceanography and ecology, Federal University of Espírito Santo, Av. Fernando Ferrari, 514 - Campus Universitário - Goiabeiras, CEP 29060-970, Vitoria (ES), Brazil

email: jacqueline.albino@ufes.br

[2]Laboratori d'Enginyeria Marítima, ETSECCPB, Universitat Politècnica de Catalunya, c/. Jordi Girona 1–3, Campus Nord ed. D1, 08034 Barcelona, Spain

email: jose.jimenez@upc.edu

[3]Environmental Engineering Department, Federal University of Espírito Santo, Av. Fernando Ferrari, 514 - Campus Universitário - Goiabeiras, CEP 29060-970, Vitoria (ES), Brazil

email: tiago.c.oliveira@ufes.br

*Corresponding author

Abstract

The Meaípe-Maimbá embayed beach (MMEB) on the south-east coast of Brazil has been subject to anthropogenic pressures since the 70's. In this study we discuss the adequacy and contribution of the parabolic planform model to determine the planform and variability of the MMEB, taking into consideration variation in wave conditions. The role of different controlling conditions on the planform variability is analyzed, as well as the morphological and planform mobility. MMEB exhibited a new configuration in response to the construction of a harbor, which interrupted the longshore sediment transport. After four decades, three particular morphodynamic sectors have been recognized along the beach. The central sector is more exposed to normal wave incidence and cross-shore processes predominate. The northern and southern sectors are influenced by wave diffraction processes around the headlands and port, respectively. In the northern sector, the presence of secondary headlands and inner islands imposed a geomorphological control on beach morphology and coastal processes. The use of the parabolic planform model provided useful insights for the assessment of potential planform mobility, since the decadal shoreline evolution combined with beach profiles and sediment characteristics allowed understanding of the beach mobility processes and supported the interpretation of modeling results.

Key words: planform modelling; geological control; beach morphodynamics; medium-term.

1 - Introduction

Understanding beach morphological variations is a major challenge for geomorphologists, coastal engineers, researchers and managers. Conceptual and numerical models for planform and cross-section equilibrium determination are widely used to analyze beach morphodynamics and to predict coastal evolution due to climate change or anthropogenic interventions (e.g. Krumblein, 1944; Hsu and Evans, 1989; Moreno and Kraus, 1999; Schiaffino et al., 2011). The parabolic model proposed by Hsu and Evans (1989) has been applied in a number of cases to study the planform of embayed beaches (e.g. Gonzalez and Medina, 2001; Klein at al., 2010; Hsu et al., 2010; Oliveira and Barreiro, 2010). Other models based on empirical mathematical functions were proposed to evaluate beach planform, namely the logaritmic spiral (Krumblein, 1944) and the hyperbolic tangent (Moreno and Kraus, 1999). The parabolic model is now the most widely adopted approach to evaluating the planform of embayed beaches. This parabolic model has the ability to predict the planform resulting from the construction of coastal structures such as breakwaters and ports, and also to determine the volume of sand needed for beach adaptation in the case of beach nourishment (Gonzalez and Medina, 2001; Hsu et al., 2010; Gonzalez et al., 2010). In addition to application in engineering projects, Oliveira and Barreiro (2010) suggest using the parabolic model to analyze embayed beach stability by comparing the existing shape with the modeled one. Schiaffino et al. (2011) modified the parabolic model proposed by Hsu and Evans (1989) in order to make it applicable to gravel beaches.

Embayed beaches are typically affected by the diffraction of waves around a headland. Therefore, three different zones are identified i) a curved portion in the zone protected from diffraction processes; ii) a slightly curved central portion; and iii) a more rectilinear distal portion (Short and Masselink, 1999; Raabe et al., 2010). A embayed beach is considered in static equilibrium when the beach shoreline is predicted by the parabolic model. Likewise, the embayed beach is in dynamic equilibrium when the predicted curve does not coincide with the actual shape (Hsu et al., 2008). However, Hsu and Evans (1989) stressed that the parabolic model could only be applied under specific conditions and is not suited to analyze every single embayed beach. One of these important conditions is that the beach should be subjected to a predominant wave direction. Short and Masselink (1999) argue that despite the evidence of diffraction processes in embayed beaches, the parabolic model does not take into account the influence of other elements of the coastal environment. There are still various factors that affect planform and beach variability besides morphodynamics, corroborating the limitations of the model. The main considerations can be summarized as: (a) planform mobility is subject to the fluctuations of the wave climate on various time scales, the processes of rotation and oscillation; (b) other processes, besides diffraction and geomorphological control, act on the development of embayed shape; and (c) there is the difficulty of adjusting the model and determine the diffraction points among multiple potential points in the area. Moreover beach profiles, sediment characteristics and wave data are needed to support planform interpretations resulting from the model.

Oliveira and Barreiro (2010) modeled embayed beaches in Portugal using the parabolic model and found discrepancies between the actual and modeled plan. Field data indicated that the beaches were in dynamic equilibrium, with the significant role of longshore sediment transport due to active longshore currents. The model suggested that beaches were in static equilibrium and the authors interpreted this result as a plan view caused by recent inversions of wave conditions and

high mobility of the beach. The parabolic model considers a predominant incident wave direction and, as a consequence, inversions of wave conditions are not considered by the model. Changes in wave climate, especially in the direction, cause variability of volume and sediment transport in embayed beaches between the two limits of the beach arc, a phenomenon known as beach rotation (Short and Masselink, 1999; Short et al., 2000). Beach rotation can occur over different timescales without changing the sediment balance (Klein et al., 2002). Medium-scale oscillations of wave direction and height would be responsible for combining cross-shore and longshore hydrodynamic and sediment transport processes (Short et al., 2000; Ranasinghe et al., 2004). Cross-shore morphological changes along an entire embayed beach are known as beach oscillation (Short and Trembanis, 2004). The combination of longshore morphological changes with cross-shore morphological changes drive the combined morphological change in a embayed beach (Harley et al., 2011).

According to Lausman et al. (2010a, 2010b), the parabolic model cannot predict the shape of the beaches in dynamic equilibrium, since it does not describe what happened up to the static equilibrium. Ranasinghe et al. (2004) proposed a conceptual model for the embayed beaches of Australia, where periods of retreat or accretion on the beach were identified under the rotational process. The temporal and spatial variability of wave heights act predominantly on the longshore and cross-shore transport to the coast. The longshore current generated by waves is responsible for different water levels and morphological processes at the embayed beach extremes. The numerous disagreements between the actual and predicted beach shapes in plan studies of the Brazilian coast were attributed to the lack of information about the submerged portion morphology and physical processes, especially in reflective beaches (Klein at al., 2010). Thus, the morphodynamic data are believed to help the interpretation and applicability of the modeled planform. However, determining the diffraction point used in the parabolic models for beaches in

equilibrium is still not a simple and straightforward task, either due to the difficulty in identifying the point among the many potential diffraction points that geomorphologically control the rocky shores, or due to the operator subjectivity. The problem of identifying the right diffraction point when shoals are present close to the headlands was discussed by Bowman et al. (2014) for beaches of Elba Island in Italy. Klein et al. (2003) argue that successful implementation is achieved only when embayed beaches are in dynamic equilibrium, and there is a precise geometrical relationship between the parabolic shape and the wave angle. The change in the diffraction and control points changes the approach angle of the wave and the modeled plan. Gonzalez (1995) pointed out other limitations when defining the control point, such as the presence of river mouths and islands. Jackson and Cooper (2010) choose multiple diffraction points to adjust the plan model to the actual configuration of some beaches of Ireland, including more internalized secondary diffraction points that receive diffracted waves. Geometric shapes as an ebb tidal delta were also considered potential diffraction points. According to these authors, the plan equilibrium concept assumes that the wave diffraction is responsible for the shaping process and all other processes are disregarded. This assumption is invalid for natural shores. However, the alternative and possible interpretation is that secondary diffraction points are not important when the predicted and actual coast are in agreement and the angle of the waves used is correct. If the coast is unstable, but the predicted and actual plans agree, the coast is subjected to oscillatory and rotational patterns that are not considered in the model. Despite the limitations in the use of the parabolic model it presents important advantages to the logarithmic spiral model and the hyperbolic tangent model. According to Hsu et al. (1987) the logarithmic spiral model should only be applied in the zone protected from the diffraction processes. Furthermore the logarithmic spiral model is not valid to be used as criterion to verify beach stability (Walton, 1977). Oliveira

and Barreiro (2010) observed that the application of the hyperbolic tangent model is not very intuitive and is more complex than the parabolic and the logarithmic spiral model.

This study applies the parabolic model of Hsu and Evans (1989) to evaluate the planform variability in the Meaípe-Maimbá embayed beach (MMEB), located in Espírito Santo, Brazil (Fig. 1). Seasonal and decadal wave changes are considered when assessing planform variability. Wave climate data of 38 years' duration are used to identify in the plan, portions of the beach susceptible to morphological adaptation. This identification is carried out considering the shape of the beach and the characteristics of the diffraction processes. The studied beach is a portion of the coast where the crystalline rock outcrops create an extremely indented coastline, with headlands and islands. In 1977, a private harbor was built in the 6 km-long beach, dividing it into two separate bay beaches. The beach probably changed from static to dynamic equilibrium to adapt to the new port structure. Today, more than 40 years from the harbor construction, it is likely to be in new static equilibrium with the prevailing incident waves. The presence of headlands, islands and shore platforms cause small arches to develop within the main embayment. Therefore, the geomorphological characteristics greatly control beach morphology and coastal processes. The beach is narrow and limited along its length by active cliffs and urban structures, which are often reached by waves, and erosion events are observed. Considering the characteristics and historical evolution of MMEB, the main objectives of this study are to discuss and evaluate: (A) the adequacy and contribution of the parabolic model of Hsu and Evans (1989) to determine the planform and variability of the Meaípe-Maimbá embayed beach in terms of changes in wave climate; (B) the role of different controlling conditions on the variability in planform; (C) the beach planform and morphological mobility. In order to achieve these objectives the potential mobility of the modeled beach plan, which takes into account the wave direction changes over 38 years, was evaluated considering contemporary morphodynamic processes.

2 - The study site

The state of Espírito Santo, in south-eastern Brazil, faces the Atlantic Ocean (Fig. 1). The Meaípe-Maimbá beach is located 70 km south of Victoria, the state capital, in Guarapari and Anchieta municipalities. Precambrian crystalline hills and Neogene sedimentary plains alternate along this portion of the coastline, forming beaches and discontinuous coastal plains. Shore platforms and beach rocks develop small beach arches along the Meaípe-Maimbá beach (Fig. 2A). The narrow sandy strip, bounded by sharp cliffs in some portions, is not wide enough to protect urban structures and erosion processes are observed in the important coastal route, Highway ES 010 (Fig. 2C). The beach is 10 km long, bordered to the north and south by the Meaípe and Ubu headlands, respectively. In 1977, the construction of a port in the southern portion divided the embayment in two distinct embayed beaches, the northern one approximately 7.7 km long. Small islands and shore platforms are present in the central portion (Fig. 1).

The sand composition of this beach is predominantly siliciclastic; however, the contribution of heavy minerals can reach up to 45% by weight on the surface level of the beach face in storm conditions when the light fraction is more easily removed (Fig. 2b, detail). The heavy fraction composition indicates that sediments derived from erosion processes of the sedimentary cliffs and weathered material from crystalline headlands are the main source of the beach sediment (Coutinho, 1974; Anjos et al., 2006). The contribution of carbonate sands generated by incrustations is more relevant in the submerged portion, where organisms such as coralline algae and mollusks on the rocky substrate are abundant (CEPEMAR, 2009).

The coastline is predominantly NE-SW oriented and exposed to the Atlantic pressure systems. The most intense winds are the E and SE winds, associated with the trade winds and the winds that arise from the passage of frontal systems, respectively. Pianca et al. (2010) proposed, based on data from the NWW3 (operational model hindcast reanalysis), that waves heights of 1 to 2 m and waves periods of 6 to 8 s coming from east are dominant during summer, winter and spring. In the fall, SE waves predominate, followed by E waves, with heights between 2 and 3 m and periods ranging from 10 to 12 s. The spring tide range in the region is 1.70 m (DHN, 2012).

3 - Methods

Three data sources were used in this study: (a) wave data, (b) topographical and sedimentological survey data, and (c) aerial photography and cartographic data. The different methods used to collect and treat the data are grouped as follows: 3.1) Waves, 3.2) Morphology and sedimentology, 3.3) Longshore sediment transport, 3.4) Shoreline variation and 3.5) Equilibrium and variability of beach planform.

3.1 Wave Data

Hindcast wave data were obtained for the period between 1970 and 2008 from the *Global Ocean Wave* (GOW) model, which consists of a reanalysis of global waves (Reguero et al., 2012). The time series of the various statistical parameters of wave and spectral energy were obtained from the GOW, which uses a global mesh with 1.5° longitude and 1.0° latitude and hourly resolution. The GOW model has been calibrated and validated globally using instrumental measurements of 21 buoys and satellite altimetry data extracted from satellite images (Reguero et al., 2012). This study uses the results given by GOW model for the 20°50'S and 40°25'W coordinates (30 m depth) between 1970 and 2008. The robustness of the GOW model to represent wave conditions near the Meaípe-Maimbá beach was analyzed. To this end, the numerical results were compared with sea

wave data obtained in situ with an Acoustic Doppler Current Profiler (ADCP) at 20°48'S and 40°33'W (25m depth) during 4 periods in the field campaign: i) 31/01/2007 to 04/04/2007; ii) 29/09/2007 to 25/10/2007; iii) 23/11/2007 to 18/12/2007; and iv) 23/11/2007 to 6/3/2008. Fig. 3 shows the comparison of the parameters, significant wave height (H_s), peak wave period (T_p) and mean direction (θ) obtained by GOW and measured in situ for the 4 periods of the field campaign. The root mean square error (RMSE) and bias for significant wave height, peak wave period and mean wave direction calculated over the 4 periods are given in Table 1.

In general the GOW model results reproduce quite accurately the evolution and magnitude trends of the parameters H_s, T_p and θ recorded *in situ*. However, it is noted that sometimes T_p and θ display episodic variations that are not correctly represented in the model. These variations are mostly associated with T_p and θ smaller than 6 s and 45°N, respectively, and therefore may be related to less energetic waves generated by local winds, not considered by the global model.

Fig. 4 shows the distribution of θ with H_s and T_p simulated by the GOW model, for the 38-year period, during which wave directions are mainly from southeast to east (63%) and northeast to east (25%). The most common ranges of wave heights are 0.5 to 1.0 m (47%) and 1.0 to 1.5 m (42%), while waves 2.0 m high and above have an occurrence probability of 1.5%. For the studied wave periods, 76.42% are between 6 and 8 s.

3.2 Morphology and sedimentology

The morphological field data were obtained in 4 surveys conducted in October 2006, February and December 2007 and February 2008, at 6 stations (P1 to P6) along the beach, as shown in Fig. 1. The cross-sections started at emerged fixed points (P1 to P6 in Fig. 1) located on the cliffs or on the narrow coastal plain and were extended around 400 m to the shoreface. A surveyor's Dumpy Level and a graduated staff were used in the topographic survey. The bathymetric part of the profiles was establish using a vessel equipped with an ODOM Hydrotrac Sounder operated at 200 kHz (accuracy of 0.01 m ± 0.1% of depth). Positioning was obtained with a DGPS (Differential Global Positioning System) with a horizontal accuracy of +/- 0.9 m. The reference level adopted as vertical datum for the surveys was 0.82 m, corresponding to the Mean Tide Level at Ponta de Ubu Terminal – Espírito Santo State (Diretoria de Hidrografia e Navegação, DHN) of the port located in the embayment.

The morphological parameters were determined based on topographic data: (a) berm height, (b) beach width (distance between the Mean Water Level (MWL) shoreline and the landward limit of the beach, corresponding to the base of the cliff or the base line on the vegetated coastal strand), and (c) beach-face slope. The superposition of beach profiles yielded an estimate of beach mobility given by the changing sediment volume. This estimation is made taking into account the beach volume above mean water level per linear meter of beach (m^3/m).

The sedimentological field data were collected on the surface level of the beach face (in the swash zone) in 5 surveys (October 2006, February, April and December 2007 and February 2008) at the same locations as the topographic profiles. The sample composition (content of siliciclastics, heavy minerals and $CaCO_3$) and particle size were determined. Size and distribution of sand fractions were determined by dry sieve analysis in 1/2 phi intervals. The sediment grain size classification

proposed by Folk (1964) was estimated using the software GRADISTAT version 4.0 (Blott and Pye, 2001). Carbonate content was determined by dissolution with hydrochloric acid. Heavy minerals were separated from light minerals by density separation using bromoform (density = 2.86 g/cc). The contents of carbonate and heavy mineral fractions were obtained by the difference between the initial and final sample weights analyzed.

3.3 Longshore Sediment Transport

The longshore sediment transport was calculated for a central beach profile using the CERC (1984) equation. This method is based on the assumption that the sediment transport is directly proportional to the longshore component of the wave energy flux, determined at wave breaking point. In the CERC equation, the value Q_l (in m^3/s) expresses the sediment transport rate by a wave of significant height, H_b, at the breaking point:

$$Q_l = K \cdot H_b^{5/2} \cdot sen(2\alpha_b) \cdot \frac{\rho\sqrt{g}}{16\gamma^{1/2} \cdot (\rho_s - \rho)(1-n)} \quad (1)$$

where ρ_s is sediment density; ρ is sea water density; n is sediment porosity; α_b is the angle between the crests of the waves breaking and the shore; K is an empirical proportionality coefficient; and g is acceleration due to gravity.

The value of K was calculated according to the equation proposed by Mil-Homens et al. (2013). These authors used a field and laboratory database (a total of 247 sampling points) to analyze K trends with respect to a large number of parameters and found that the best fit for K is obtained by the polynomial function:

$$K = \left[2232.7\left(\frac{H_b}{L_0}\right)^{1.45} + 4.505\right]^{-1} \quad (2)$$

where, L_0 is the deep water wave length. Propagation based on linear wave theory was used in this study to propagate 30 m-deep waves to the onshore breaking point. This method accounts for shoaling and refraction, and is based on Snell's law, the wave energy conservation principle and the assumption that waves propagate on a constant sloping bathymetry parallel to the shoreline. The depth-induced wave breaking criteria H/h = 0.78 (McCowan, 1894) is used to identify the breaking point. Calculations consider ρ_s= 2600 kg/m^3, ρ = 1025 kg/m^3 and g = 9.8 m^2/s.

3.4 Shoreline variation

The shoreline evolution was determined by superimposing the shorelines extracted from aerial photographs from 1970 and 2008. The 1970 scanned coastline, 1:35000 scale, was provided by the Instituto de Defesa Agropecuária e Florestal do Espirito Santo (IDAF-ES). The geo-referenced aerial photo of 2008, scale 1:8000 was courtesy of the Instituto Estadual de Meio Ambiente (IEMA-ES). Both photos have a georeferencing precision of 1 m. The 2008 coastline photo was scanned and overlapped with the 1970 photo using the GIS software package Arcgis 9.3® to datum WSG 84, scale 1:3000. The DSAS 4.0 (Digital Shoreline Analysis System) software was used to calculate shoreline variation using 39 cross-sections along the beach, separated by 200 m from each other. The location of the shoreline was defined based on the previous high tide high water level (Boak and Turner, 2005). As a basic approximation, considering a 1:8 reflective slope with 1.7 m tide range, we can assume a lateral error of about 6.8 m on the shoreline detection.

3.5 Equilibrium and variability of beach planform

In polar coordinates, the parabolic bay equation developed by Hsu and Evans (1989) is given by:

$$\frac{R}{R_0} = C_0 + C_1\left(\frac{\beta}{\theta}\right) + C_2\left(\frac{\beta}{\theta}\right)^2 \quad (3)$$

where *R* is the length between the control point (diffraction point) and any point on the bay periphery, R_0 is the control line length (where the linear zone of the shoreline starts), β is the wave obliquity, C_0, C_1 and C_2 are coefficients defined empirically depending on β. In this work the application of the parabolic equation was performed using the software MEPBAY (Klein et al., 2003).

According to Hsu and Evans (1989) and Hsu et al. (2008), certain conditions must be met for successful implementation of the parabolic model and its suitability in equilibrium assessment, namely: (a) the beach should be predominantly composed of sand, (b) the beach should be subjected to a predominant wave direction; (c) the beach must be submitted to micro-tidal regime; (d) there must be a headland that represents the diffraction point; (e) cross-shore sediment transported during storm events, forming bars, must return to the beach face under fair weather conditions; (f) the wave incidence angle should produce a longshore current and be associated with prevailing waves; and (g) the resultant of the annual longshore sediment transport is higher than the resultant from storm sediment transport.

Hsu et al. (2008) interpret and classify the results of the comparison between the actual and modeled shape as follows:

• If the embayed beach shoreline is predicted by the parabolic equation, the beach is considered in static equilibrium. The straight outer portion is parallel to the wave crests approaching the

shore. To meet this requirement, it is assumed that no sediment is added or eroded from the embayed beach in the future; wave conditions are maintained and persistent; waves break simultaneously along the beach and longshore drift is almost nonexistent.

• If the predicted shoreline is located landward in relation to the actual shoreline, the beach section is considered to be in dynamic equilibrium and is susceptible to erosion resulting from changing available sediment or wave climate. Furthermore, the beach is classified as "natural beach reshaping" when in the shadow area, protected by a headland or engineering structure, the shoreline progrades and is more exposed to erosion. The eroded sediments are carried by the longshore drift up to the protected portion. The parabolic model requires that the diffraction points and control point be chosen on a plan over an aerial photograph (Klein et al., 2003).

Based on the aerial photo of 2008 (scale 1:8000) and the wave climate between 1970 and 2008, the planform equilibrium was evaluated for two conditions. Firstly, the planform was evaluated considering the average wave direction between 1970 and 2008 as a predominant wave direction. In this study, we refer to this average wave condition as ‘representative wave’. Secondly, the planform was evaluated considering a wave direction that is obtained based on the assumption that the beach from the aerial photo of 2008 is in static equilibrium. In other words, a geomorphological wave fitting to the parabolic model is done. Hereinafter, we term this wave condition as ‘geomorphological wave’.

The Meaípe-Maimbá beach has distinct diffraction points to the north and south ends. To the south, the diffraction point is represented by the breakwater head of the port. To the north, it is represented by headlands and crystalline islands. In this case all the potential diffraction points were taken into account in order to evaluate the embayment planform. The inner island in the north part of the beach was considered as a secondary diffraction point.

Potential oscillations of the beach planform induced by changes in the incident wave angle were analyzed. The mobility of the beach was determined by introducing the variation of the annual averaged wave direction between 1970 and 2008 in the model.

4 Results

4.1 Beach Mobility

4.1.1 Variation of the shoreline in recent years

From 1970 to 2008, the comparison between the shoreline plans from transects 34 to 39 (Fig. 5) showed an average progradation of 121.89 m in the southern portion of the beach. This totals an increase of 122,000 m^2 in area in the last 38 years, which corresponds to a rate of 3200 m^2/year. An average retreat of 15 m is observed along the northern and central portion of the beach between transects 1 and 33. In the northern portion of the beach (between transects 1 and 13) the shoreline was more stable, with an average 13 m shoreline retreat. The central portion (between transects 14 and 33) presents retreat values that range from 17 to 28 m. The total erosion in the northern and center portions is 99,000 m^2 in area, which corresponds to a rate of 2600 m^2/year. The long-term balance of the beach is positive with a progradation rate of 600 m^2/year.

Assuming that the Meaípe-Maimbá beach is a closed system, the small difference between retreat and accretion can be explained partially by the area of progradation being a plain beach. By contrast, vertical variation in the cliffs portion of the beach is considered to have occurred without significant horizontal variation. These discrepancies between accretion and retreat were observed

by Lausman et al. (2010b) for other Brazilian beaches. The erosion processes that increase the sediments eroded from the cliff and transported across the beach may explain the difference observed.

The port, built in 1977, became a barrier to the longshore transport of the sand. This barrier is responsible for the largest width of the south beach, and the vegetated and stable coastal plain recently developed between the cliffs and the active beach. The north-central beach is directly backed by the cliffs (Fig. 2) and narrow coastal plains are observed among the small arches.

The beach has shown little mobility and changes in the plan are most noticeable in the long term. It is likely that the morphological adaptation was faster and more intense in the early years, soon after the port construction. Thus, it is assumed that the beach has experienced lower mobility in recent years.

4.1.2 The modeled shape and plan mobility

Table 2 presents the results for the annual longshore sediment transport (Equation 1) and K values (Equation 2) obtained for 2008 as a reference year. Results indicate a residual transport of 396,754 m^3/year, directed southwards.

The direction of the representative wave, responsible for the beach planform during the 38 year period, is 113°N (i.e. ESE). The wave climate was considered stable, with a small fluctuation of ± 4° in the annual mean direction (Fig. 6). This small fluctuation in wave direction strengthens the resultant from the sediment transport from north to south (Table 2). Moreover an increase in the incident wave energy from 1996 onwards (Fig. 6) suggests an increase in capacity to mobilize sediments.

Considering the morphology and degree of exposure to incident waves, Maimbá beach can be divided into three sectors, (a) the curved northern sector subjected to wave diffraction processes around the headlands and island; (b) the straighter central sector exposed to the incident waves and limited by the cliffs; and, (c) the curved southern sector controlled by the wave diffraction processes around the port. The central sector also indicates the geomorphological control imposed by the presence of eroded cliffs. Furthermore, the parabolic model indicated wave diffraction process in the northern and southern sectors, with final control in the central sector (Fig. 7).

In the northern sector, assuming a geomorphological wave condition, we observe that the modeled planform agrees with the actual shore, indicating geomorphological fitting (Fig. 7, black line). The results showed that the overall configuration is controlled by the direction of the waves diffracted by the main headland. However, small arches are produced by the processes resulting from secondary features, such as sandstones and minor headlands, while the island plays a major role. Therefore two diffraction points were taken into account in order to predict the shoreline plan. They are the main headland and the inner island in the north part of the beach. Fitting parameters that solve the parabolic bay model for Meaípe-Maimbá Beach are summarized in Table 3. The modeled shape by adopting a geomorphological wave indicates that the northern sector responds appropriately to the parabolic model and the beach is in static equilibrium.

On the other hand, the shoreline modeled using the direction of the representative wave diffracted around the main headland fits very poorly the actual shoreline. The offset between the two angles is 17° south, indicating the necessary geomorphological fitting when no final control point allows us to fit a parabolic shape. This is replaced by another process, such as the transport of sediments along the coast (Fig. 7). Considering that the beach planform is in static equilibrium,

variations in incident wave direction can induce sediment transport redistribution and modifications in the planform.

The application of the model was repeated adding to the geomorphological wave direction the variation of ± 4° found in the annual mean direction. Fig. 7 shows the potential oscillations of the beach planform induced by changing the wave angle. The innermost shoreline is associated with the wave displacement angle to the NE, thus generating increased sediment transport southwards. In this condition, the beach would be in dynamic equilibrium. On the other hand, the outer shoreline would be produced by increasing the wave angle from the SE, decreasing sediment transport to the S and resulting in a natural reshaping beach. A maximum plan mobility displacement of 141 m was obtained due to variations on wave direction.

The planform of the southern sector (see Fig. 8), whose wave diffraction point is the breakwater head of the port built in 1977, revealed that this portion of the beach is in static equilibrium with respect to representative waves in almost the entire length of the beach arc. However the shoreline is landward of the modeled shoreline in the southern extreme of the beach arc. In order to understand this difference, the presence of a secondary diffraction point provided by the ship berth jetty was tested in the model. No good fit was obtained considering this secondary diffraction point. The difference between modeled and observed shoreline can be attributed to local variations on morphodynamics processes induced by harbor dredging activities.

The application of the model was repeated in the southern sector adding to the representative wave direction the variation of ± 4° (Fig. 8b). Results indicate a maximum plan mobility displacement of 99 m in the south sector. This result indicates that the maximum plan mobility displacement is smaller in the southern sector than in the northern sector of the beach.

4.2 Beach morphology and sedimentology

4.2.1 Beach profiles

The mean values of the morphological parameters for the beach profiles are summarized in Table 4. Results indicate that the emerged width beach ranged from 23.56 m to 38.36 m between October 2006 and February 2008, in P1 and P5 profiles, respectively. The height of the berm crest ranged from 1.44 to 4.10 m above MWL, with a maximum in P5. The emerged profiles are narrow and steep due to these characteristics. The beach becomes wider, with higher berm crest height and higher gradient of the beach face southwards, from profiles P1 and P2 in the north to P5 and P6 in the south.

Beach mobility in the medium term is represented by the variations observed between October 2006 and February 2008 (Fig. 9). The surveys were conducted under easterly wave conditions, with low mobilization and transport competence. Accumulated wave energy in the last 30 days preceding each survey showed that in October 2006 the wave energy were above monthly average accumulated wave energy in 2006 (Table 5). The higher offset from the yearly average wave direction was recorded in the survey performed in December 2007, with waves from 96ºN prior to the survey. Higher wave energy variations observed between October 2006 and February 2007 reflected a significant morphological adaptation. Lower wave energy variations, observed from December 2007 to February 2008, induced more stable profiles despite the possibly sediment transport to the bay due to cross-shore transport promoted by the easterly waves (Fig. 9).

Major morphological changes were observed between October 2006 and February 2008 in profiles P1, P2, P3 and P6. These profiles are more dynamic since they aggregate processes associated with beach curvature and longshore drift. Around P4, where the sediment transported by the longshore drift moves either southwards or northwards, the cross-shore transport controls the morphology. There is also significant mobility of the nearshore bars.

4.2.2 Sedimentology

Sediment characteristics along each of the beach profiles are summarized in Table 6 and Fig. 10. The beach sediments consist mainly of siliciclastic sands and heavy minerals. The contribution of carbonate sands is less than 1% of total weigh. According to the median grain size diameter (D_{50}), the sediment is classified as medium sand, moderate to well sorted and presenting a symmetric distribution along the beach. An exception was a negative asymmetry obtained in sands of P1. The highest contribution of coarse sands is present in P4, P5 and P6.

The heavy mineral contents are higher in the north-central portion of the beach, in the beach face. The levels decrease as the sand becomes coarser to the south. The high levels of heavy minerals can be explained by the proximity to the source area, represented by crystalline headlands and sediments eroded from the sedimentary cliffs, as the higher concentration of heavy minerals is found in the proximity of such features.

The sedimentological data combined with morphological characterization allows us to classify the beach type as reflective according to Wright and Short (1984). In this case, the beach is composed of medium and coarse sands, narrow cross-sections and high profile gradients.

5. Discussion

5.1 Adequacy of the plan model and beach mobility

The Meaípe-Maimbá embayed beach presents itself as a closed cell, where over the last 4 decades the port structure interrupted the longshore sediment transport from the northern and central portion of the beach towards the southern extremity. On a decadal scale, the beach is nowadays in equilibrium with the incident waves, and current mobility is small. Three morphodynamic sectors were recognized based on mobility (Fig. 11).

The northern and southern sectors are influenced by the wave diffraction processes around the headlands and exhibit the greatest mobility, especially in the curves and near the headlands. As the beach curvature diminishes, the volume and width changes of the beach profiles are more homogeneous, as shown by Klein et al. (2002) in other beaches. In the central sector the beach becomes more stable and the cross-shore transport more active.

The parabolic model was used to determine the mobility potential of beach northern and southern sections when facing small fluctuations in the wave direction (between -4° and +4°), on a decadal scale. But the procedures for applying the model and the responses were different for the two extremes.

With only one potential diffraction point and using the representative wave on a decadal scale, the beach planform of the south beach sector was in static equilibrium. The mobility represented by volume fluctuations of the profiles (ΔV in Fig. 11) agrees with the decadal and modeled changes. Plan mobility displacement and profile variations were higher at the beach extremes while in the central portion and both scales, these fluctuations were smaller (Fig. 11).

In the southern sector, maximum plan mobility is 99 m. Regarding the current shoreline, the displacement would be higher in the case of shoreline retreat, promoted by a higher proportion of E and SE waves (a variation of +4° in wave direction) that transport sediments by longshore drift to the north. Under this condition, the waves would reach the coastal plain, feeding into the active coastal system the sediments deposited during the last 38 years. With the increase of NE waves, the modeled shoreline becomes closer to the present shoreline. Stability, observed also in the contemporary morphodynamic behaviour, would be associated with mobilization of sediment available along the active profiles.

The sediment transported by the longshore drift since the construction of the port was sufficient for the morphological adaptation of the beach arc in the south sector. The consideration of the wave direction changes in the model reflected the probable short-term morphological variation and this is, likely, in agreement with profiles' mobility. The morphological response would be stability or, if there were no sediment available, shoreline retreat.

Shoreline retreat of the northern sector would be higher under increasing NE waves (a variation of -4° in wave direction). The real magnitude of the erosion process depends on sediment availability and the existence of obstacles that limit free morphological evolution. Currently, this section is characterized by a narrow beach and limited by urbanization often exposed to wave action. The medium term sediment balance is negative (ΔV total in Fig. 11).

5.2 Beach planform and morphological mobility

The historical development shows that the southern sector of the embayed beach is in gradual accretion and the northern sector in progressive retreat. This can be explained by the potential longshore sediment transport of 400,000 m^3 per year, of which 95% is southwards. The longshore sediment transport is also responsible for the spatial distribution of the heavy mineral contents due to a selective removal of the hydraulically most susceptible grain sizes (Rao, 1957; Komar and Clemens, 1986; Li and Komar, 1992, among others). When the profile is subjected to erosive processes, the heavy sediment fraction tends to remain as a residual deposit (Frihy and Komar, 1993; Frihy and Dewindar, 2003). In the study area heavy mineral content is extremely variable, with highest concentrations in the northern half of the beach arc (Table 6). Mean grain size trend, with the finest mean grain size and negative skewness at P1, increases in mean size from P1 to P6 (Table 6), contrary to the expected pattern due to the grain size selective longshore transport related to the wave incidence. This increase occurs inside the same grain size classification and seems related both to an overpassing of coarser and lighter grain sizes over smaller heavier ones (Orford et al. 1991; Isla, 1993; Horn & Walton, 2007), as also an increase in wave exposure due to the configuration of the beach arc - resulting in an continuous increase in beachface declivity, increase in beach berm high (Table 4), and also in a better grain size selection toward the southern extremity of the beach.

The different geomorphological sectors of the beach and the potential energy of the waves allow considering the combined oscillating-rotating processes acting along the beach, as suggested by Ranasinghe et al. (2004). In Meaípe-Maimbá beach rotation mechanisms are suggested by the inverse behavior of volume fluctuations for the profiles (ΔV in Fig. 11) in the extremes of the embayment. In the central beach, cross-shore processes predominate, which is reflected by the profiles' mobility and grain size variation.

Despite the dominant longshore transport southwards, historical evolution analysis indicated that the northern sector is in slow progressive retreat. Seasonal sediment transport causes oscillation and rotation of the beach morphology and retards the decadal historical trend, provided that the wave variations remain. Thus, the modeled displacement would not be achieved. According to the modeled planform, the southern beach is susceptible to retreat with increasing SE waves (a variation of +4° in wave direction). Field monitoring data indicate that the beach is in equilibrium with the sediment amount present on the beach and coastal plain. Very likely over time, the beach will not attain dynamic equilibrium classification provided that sediment amount remains or even increases. Modeled results show that an increase in the frequency of NE waves leads to an increase in the potential plan mobility in the northern sector. Additionally, measured beach profiles indicate high mobility in the north sector. This sector still does not have sufficient sediment for future adaptations. The sandy beach is narrow and bordered by either active cliffs or urban structures. The cliffs can be potential sediment sources, but causing loss of area for urbanization (Fig. 2). The reclassification of the beach in dynamic equilibrium due to changes in the amount of sediment and/or wave variation is observed in the northern sector. However, modeled displacements can be overestimated due to the fact that the model doesn't take into account medium term processes and some geomorphological features.

Depending on the duration of the analyzed period, the intensity of coastal processes can be fundamental in explaining the final planform. In other words, the time required for wave changes can be shorter than that required for planform adaptation. But it is likely that the beach dynamics respond quickly to medium-term changes, as seen for the Meaipe-Maimbá beach and the Portuguese beaches studied by Oliveira & Barreiro (2010), where there was disagreement with the current wave dynamics.

5.3 The geomorphological control on the implementation of the plan model and beach mobility

Different factors limit the application of the planform beach model (Hsu and Evans, 1989). Among these factors, two were identified in the northern section of Meaipe-Maimba beach: (i) other processes, besides diffraction and geomorphological control, act on the development of embayed shape and (ii) difficulty of adjusting the model and determine the single diffraction point among potential points. Assuming that the representative wave is correct, the planform is inadequate in the northern sector (Fig 7a), since secondary processes produce uncertainty in the application, as proposed by Gonzalez (1995). In the southern sector, the beach is in static equilibrium with respect to the representative wave in almost the entire length of the beach arc.

According to Klein et al. (2003), the parabolic model is successful only for beaches in static equilibrium. Considering, on the one hand, that the Meaipe-Maimba beach plan is in equilibrium in the aerial photo and, on the other, the existence of two diffraction points (the main headland and the inner island), it was found that the modeled planforms fit the current shoreline. A similar approach was used by Jackson and Copper et al. (2010) to model the planform of natural beaches in Northern Ireland. Fitting the modeled planform to the current configuration exposes the method to subjectivity (e.g. Lausman et al., 2010 a, 2010 b; Klein at al. 2010). However, this

procedure was satisfactory used in the assessment of potential planform mobility in this study. Decadal shoreline evolution combined with beach profiles and sand sedimentary data improved the current understanding of MMEB morphodynamic behavior. Moreover the available data supported the interpretation of modeling results. The need for beach profiles and sedimentary data to analyze the model plan was previously pointed by Short and Masselink (1993).

6. Conclusion

There is consensus regarding the existence of a large number of conceptual issues that may interfere with the parabolic model when compared to existing shoreline, among these, the ability of the beach to adjust to changes in wave energy and direction. The absence of dynamic variables such as currents, sedimentology and shoreface morphology limits its application.

In this study, the parabolic model was applied to evaluate the mobility potential of the Meaípe-Maimbá embayed beach due to wave changes over a period of 38 years, considering that the beach is in static equilibrium. Information about shoreline evolution trend and seasonal profile variability was fundamental for the successful interpretation of the results. However, the displacement modeled by the parabolic model did not show the magnitude and intensity of erosive behavior along the beach. The pace of the adjustment depends on sediment availability and, especially, on short-term sediment transport processes.

Local geomorphological control acts on the resulting beach planform, since it limits sediment transport along the beach and influences local wave dynamics. It is not a simple task to identify the diffraction and control points among the potential ones and achieve, by modeling, the resulting planform of the beach in equilibrium. Nevertheless, assuming that the beach is in static equilibrium under the condition of incident waves, the mobility can be modeled in terms of changes over time and this application may be considered a useful tool in coastal management.

Acknowledgements

The first author acknowledges the support of the CNPq for granting the post-doctoral scholarship, process 200047/2011-6. The third author acknowledges the post-doctoral scholarship provided by CAPES, contract number A039_2013. Thanks are due to Samarco Mineradora S.A. and CEPEMAR - Serviços de Consultoria em Meio Ambiente Ltda for providing the wave buoy data, bathymetric and sedimentological data of the beach, and to Reguero et al. (2012) for the modeled wave data. We are grateful to the reviewers of this paper for critical evaluation and valuable suggestions. This manuscript is a contribution to INCT-MAR Ambitropic research project(CNPq).

Table caption

Table 1 - Mean error statistics for the hindcast data of significant wave height (Hs), peak wave period (Tp) and Mean Wave Direction (θ).

Table 2 - Longhore sediment transport along the Meaípe-Maimbá beach, in 2008.

Table 3 - Fitting parameters that solve the parabolic bay model in the Meaípe-Maimbá Beach.

Table 4 - Mean values of profile morphological parameters.

Table 5 - Average wave direction (θm) and accumulated wave energy (τm) of 30 days prior to survey. Yearly average wave direction (θyear) and monthly average accumulated energy (τ/12) in the survey year.

Table 6 - Mean values of sedimentological parameters based on 5 field campaigns (Oct '06, Feb '07, Apr '07, Dec '07 and Feb '08)

Figure caption

Figure 1 - Map showing Maimbá Beach and distribution of sampling stations (P1 to P6). (A), (B, (C) and (D) position of photos in Figure 2.

Figure 2 - (A) Active sedimentary cliffs in the central sector of the Meaípe-Maimbá beach, ES; (B) shore platforms, beach rocks and high concentration of heavy minerals near sampling station P3; (C) erosion of the Neogene deposits in the vicinity of the coastal highway near P2 (Photos: December 2007); (D) Rubble-mound revetment (Photo: October 2012). View position in Fig.1.

Figure 3 - Comparison of the parameters, significant wave height (H_s), peak period (T_p) and mean direction (θ) given by GOW and measured in situ for the 4 periods of field campaign.

Figure 4 - Directional histograms of wave characteristics according to the GOW model. Left: wave height; Right: Wave period.

Figure 5 - Evolution of the shoreline in 38 years.

Figure 6 - Variability of annual mean wave direction ($\Delta\theta$, solid line) and cumulative annual energy ($\tau=H^2T$, dot line), between 1970 and 2008.

Figure 7 - North sector of Meaípe-Maimbá embayed beach: (a) Planform modeled with waves adjusted to the coast in static equilibrium (black) and to the representative wave (white); (b) potential mobility as a function of seasonal variation in the direction of incident waves, where the innermost shoreline is associated with -4° change (NE) and the outermost shoreline with +4° change (SE).

Figure 8 - South sector of Meaípe-Maimbá embayed beach: (a) Planform in static equilibrium; (b) potential mobility in plan in terms of wave direction fluctuations. Inner line, increment of (+4°) SE waves.

Figure 9 - Morphological variation of the transversal profiles along the Meaípe-Maimbá embayed beach (see Figure 1 for profiles location).

Figure 10 - Grain size distribution and heavy mineral concentration.

Figure 11 - Planform and profile mobility. Profile mobility is represented by the change in volume profiles (ΔV) of October ‘06 (1), February ‘07 (2), December ‘07 (3) and February ‘08 (4). Modeled plan mobilit is identified by shorelines displacements (plan mobility displacement) induced by changes in wave direction (+/- 4°). Solid line = progradation, dotted line = retreat.

References

Anjos, R.M., Veiga, R., Macario, K., Carvalho, C., Sanches, N., Bastos, J., Gomes, P.R.S., 2006. Radiometric analysis of Quaternary deposits from the southeastern Brazilian coast. Marine Geology, 229, 29-43.

Blott, S.J., Pye, K., 2001. Gradistat: a grain size distribution and statistics package for the analysis of unconsolidated sediments. Earth Surface Processes and Landforms 26 (11), 1237–1248

Boak, E.H.; Turner, I.L., 2005. Shoreline Definition and Detection: A Review. Journal of Coastal Research, 21, 4, 688-703.

Bowman, D., Rosas, V., Pranzini, E., 2014.The pocket beaches of Elba Island (Italy) - Planview geometry, Depth of closure and sediment dispersal. Estuarine Coast and Shelf Science, 136: 37-46.

CEPEMAR Serviços de Consultoria em Meio Ambiente Ltda, 2009. Estudo Hidrodinâmico da área de influencia do Porto de Ubu. Samarco Mineração. Relatorio Técnico CPM RT 373/09. Vitoria, ES Brazil.

CERC, 1984. Shore Protection Manual, vols. I and II. Coastal Engineering Research Center, USACE, Vicksburg.

Coutinho, J.M.V., 1974. O Pré-Cambriano do Vale do Rio Doce como fonte alimentadora de sedimentos costeiros. In: XXVIII, Anais Congresso Brasileiro de Geologia 5, 43-56.

Del Valle, R., Medina, R., Losada. M., 1993. “Dependence of coefficient k on grain size”, Technical Note No. 3062. Journal of Waterway, Port, Coastal and Ocean Engineering, Vol 119, No. 5.

Diretoria de Hidrologia e Navegaçao – DHN. 2012 Tábua de Marés. Terminal da Ponta de Ubu – Estado do Espírito Santo. Marinha do Brasil.

Folk, R.L., 1974. Petrology of sedimentary rocks. Hemphill, Austin, Tex., 182p.

Frihy, O.E., Komar, P.D., 1993. Long-term shoreline changes and the concentration of heavy minerals in beach sands of the Nile delta, Egypt. Marine Geology 115, 253-261.

Frihy, O.E.,Dewidar, K.M., 2003. Patterns of Erosion/sedimentation, heavy mineral concentration and grain size to interpret boundaries of littoral sub-cells of the Nile Delta, Egypt. Marine Geology 199, 27-43.

Gonzalez, M., 1995. Morfologia de playas en equilibrio: planta y perfil. PhD Thesis, Departamento de Ciencias y Tecnicas del Agua y del Medio Ambiente. Universidad de Cantabria. Santander, Spain.

Gonzalez, M., Medina, R., 2001. On the application of static equilibrium bay formations to natural and man-made beaches. Coastal Engineering 43 (3-4), 209-225.

Gonzalez, M., Medina, R. Losada, M., 2010. On the design of beach nourishment projects using static equilibrium concepts: Application to the Spanish coast. Coastal Engineering 57, 227-240.

Harley, M.D., Turner, I.L., Short, A.D., Ranasinghe, R., 2011. A re-evaluation of coastal embayment rotation: the dominance of cross-shore versus alongshore sediment transport processes in SE Australia. Journal of Geophysical Research 116 (F04033), 16 http://dx.doi.org/10.1029/2011JF001989.

Horn, D.P; Walton S.M., 2007. Spatial and temporal variations of sediment size on a mixed sand and gravel beach. Sediment. Geology 202 (3):509-528.

Hsu, J,R.C., Silvester, R., Xia, Y.M., 1987. New characteristics of equilibrium shaped bays. Proc. 8th Aus. Conf. Coastal and Ocean Eng., 140-144.

Hsu, J.R.C., Evans, C., 1989. Parabolic bay shapes and applications. Proceedings of the Institute of Civil Engineers, Part 2, vol. 87, 557-570.

Hsu, J.R.C., Lee, F.C., Benedet, L., 2010. Static bay beach concept for scientists and engineers: a review. Coastal Engineering 57, 76-91.

Hsu, J.R.C., Benedet, L., Klein, A.H.F., Raabe, A.L.A., Tsai, C.P., Hsu, T.W., 2008. Appreciation of static bay beach concept for coastal management and protection. Journal of Coastal Research 24, 198-215.

Isla,F.I. 1993. Overpassing and armouring phenomena on gravel beaches. Mar Geology 110 (3-4):369-376.

Jackson. D.W.T., Cooper, J.A.G., 2010. Application of the equilibrium planform concept to natural beaches in Northern Ireland. Coastal Engineering 57, 112-123.

Klein, A.H.F., Ferreira, O., Dias, J.M.A., Tessler, M.G., Silveira, L.F., Benedet, L., Menezes, J.T., Abreu, J.G.N., 2010. Morphodynamics of structurally controlled headland-bay beaches in southeastern Brazil: a review. Coastal Engineering 57, 98-111.

Klein, A.H.F., Vargas, A., Raabe, A.L.A., Hsu, J.R.C., 2003. Visual assessment of bayed beach stability wit computer software. Computers and Geosciences 29, 1249-1257.

Klein, A.H.F., Benedet, L., Schumacher, D.H., 2002. Short-term beach rotation processes in distinct headland bay beach systems. Journal of Coastal Research 18, 442-458.

Komar, P.D., Clemens, K.E., 1986. The relationship between a grain's settling velocity and threshold of motions under inidirectional currents. Journal of Sedimentary Petrology 56, 258-266.

Krumblein, W.C., 1944. Shore processes and beach characteristics. Technical Memorandum N°3, Beach Erosion Board, U.S. Army Corps Engineers. 47 pp.

Lausman, R. Klein, A.H.F., Stive, M., 2010a. Uncertainty in the application of Parabolic Bay Shape Equation: Part 1. Coastal Engineering 57, 132-141.

Lausman, R. Klein, A.H.F., Stive, M., 2010b. Uncertainty in the application of Parabolic Bay Shape Equation: Part 2. Coastal Engineering 57, 142-151.

Li, M.Z; Komar, P.D., 1992. Selective entrainment and transport of mixed size and density sands; flume experiments simulating the formation of black-sand placers. Journal of Sedimentary Research 62 (4), 584-590.

McCowan J., 1894. “On the Highest Wave of Permanent type,” Phil Mag J Sci, Vol 38, pp.351-358.

Mil-Homens J. , Ranasinghe R. , van Thiel de Vries J.S.M. , Stive M.J.F., 2013. Re-evaluation and improvement of three commonly used bulk longshore sediment transport formulas, Coastal Engineering 75, 29-39.

Moreno, L.J., Kraus, N.C., 1999. Equilibrium shape of headland-bay beaches for engineering design. Proceedings Coastal Sediments '99: American Society of Civil Engineers, vol.1, pp. 860–875.

Oliveira, F.S.B.F., Barreiro, O.M., 2010. Application of empirical models to bay-shaped beaches in Portugal. Coastal Engineering 57, 124-131.

Orford, J.D., Carfter, R.W.G. and Jennings, S.C., 1991. Coarse clatic barrier environments: Evolution and implications for Quaternary sea level interpretation. Quaternary International, 9, 87-104.

Pianca, C., Mazzini, P.L.F., Siegle, E., 2010. Brazilian offshore wave climate base don NWW3 reanalysis. Brazilian Journal of Oceanography 58(1), 53-70.

Raabe, A.L.A., Klein, A.H.F., González, M., Medina, R., 2010. MEPBAY and SMC: Software tools to support different operational levels of headland-bay beach in coastal engineering projects. Coastal Engineering 57, 213-226.

Ranasinghe, R., McLoughlin, R., Short A., Symond G., 2004. The Southern Oscillation Index, wave climate, and beach rotation. Marine Geology 2004, 273-287.

Rao, C.B., 1957. Beach erosion and concentration of heavy mineral sands. Jour. Sed. Petrol.27,143-147.

Reguero, B.G., Menéndez, M., Méndez, F.Z., Mínguez, R., Losada, I.J., 2012. A Global Ocean Wave (GOW) calibrated reanalysis from 1948 onwards. Coastal Engineering 65, 38-55.

Schiaffino, C.F., Brignone, M., Ferrari, M., 2011. Application of the parabolic bay shape equation to sand and gravel beaches on Mediterranean coasts. Coastal Engineering, 59:57-63.

Short, A.D., Masselink, G., 1999. Embayed and structurally controlled beaches. In: Short, A.D. (Ed.) Handbook of Beach and Shoreface Morphodynamics. Wiley, New York, 230-249.

Short, A.D., Trembanis, A.C., Turner, I.L., 2000. Beach oscillation, rotation and the Southern Oscillation, Narrabeen Beach, Australia. Proceeding Coastal Engineering, 2000, 2439-2452.

Short, A.D., Trembanis, A.C., 2004. Decadal scale patterns in beach oscillation and rotation Narrabeen Beach, Australia--time series, PCA and wavelet analysis. J. Coast. Res, 20(2), 523-532.

Walton, T.L., 1977. Equilibrium shores and coastal design. Proceedings of Coastal Sediments '77, ASCE, pp. 1–16.

Wright, L.D., Short, A.D., 1984. Morphodynamic variability of surf zones and beaches: a synthesis. Marine Geology 56, 93–118.

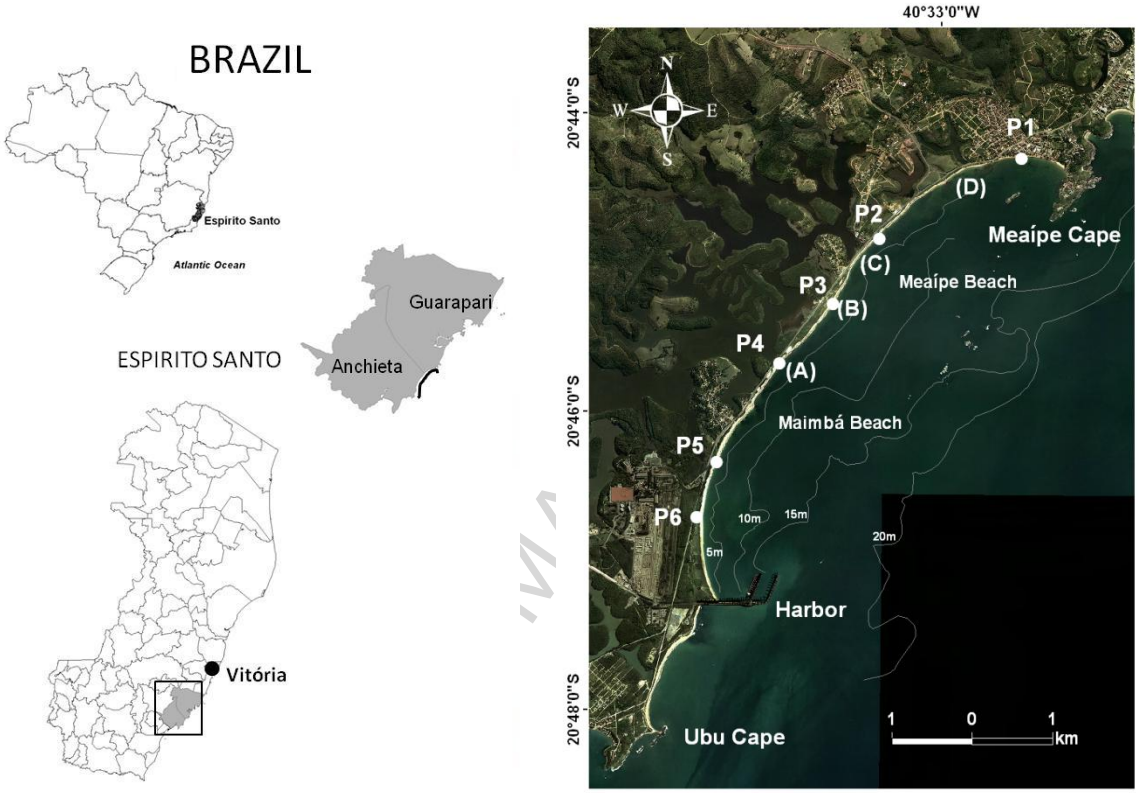

Figure 1: Map showing Maimbá Beach and distribution of sampling stations (P1 to P6). (A), (B, (C) and (D) position of photos in Figure 2.

Figure 2: (A) Active sedimentary cliffs in the central sector of the Meaípe-Maimbá beach, ES, (B) Shore platforms, beach rocks and high concentration of heavy minerals near sampling station P3, (C) Erosion of the Neogene deposits in the vicinity of the coastal highway near P2 (Photos: December 2007); (D) attempted containment (Photo: October 2012). View position in Fig.1.

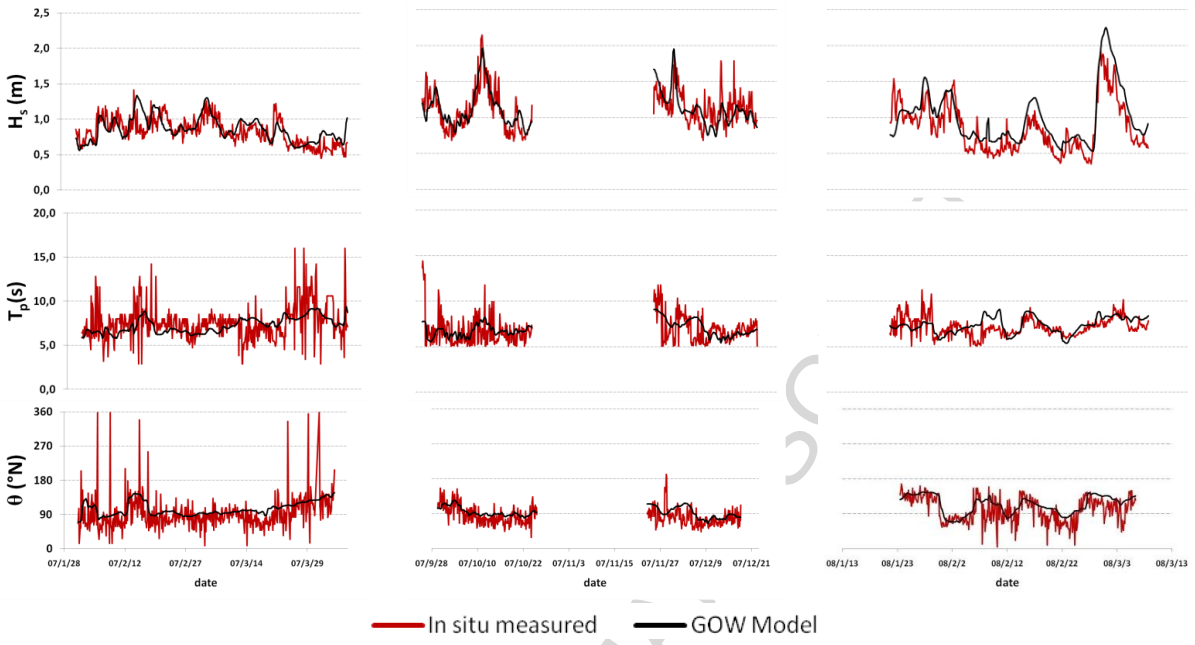

Figure 3 - Comparison of the parameters, significant wave height (H_s), peak period (T_p) and mean direction (θ) given by GOW and measured *in situ* for the 4 periods of field campaign.

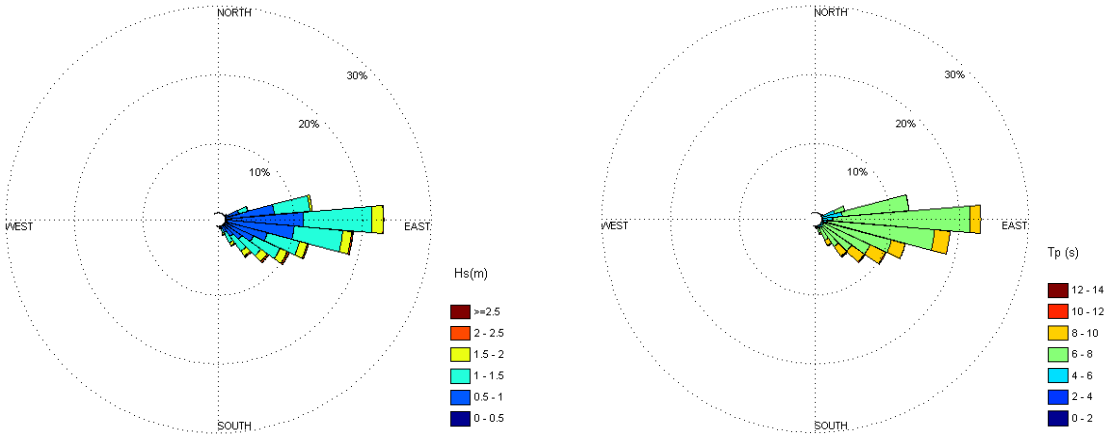

Figure 4. Directional histograms of wave characteristics according to the GOW model. Left: wave height; Right: Wave period.

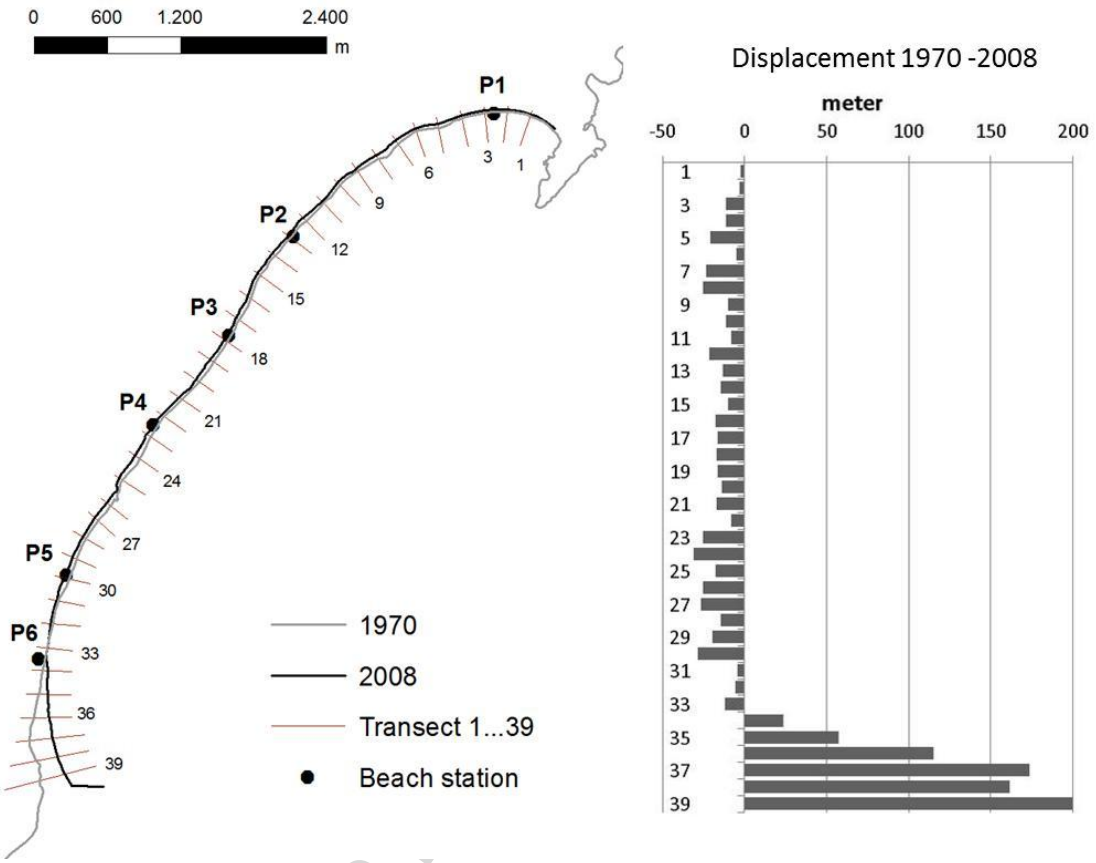

Figure 5: Evolution of the shoreline in 38 years.

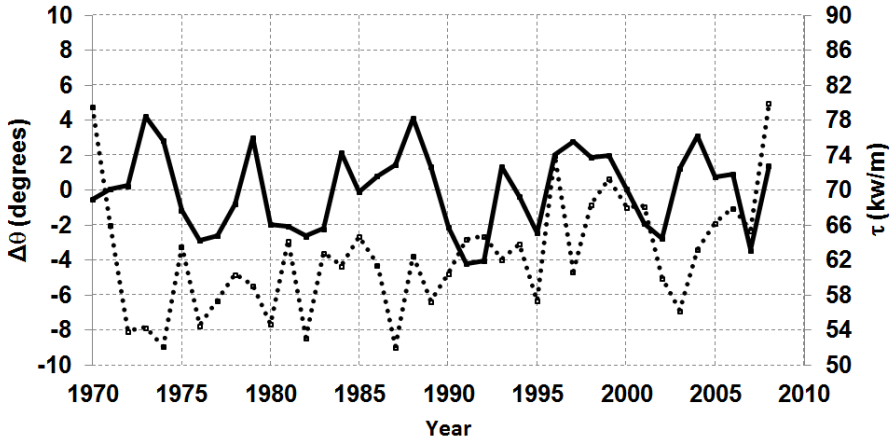

Figure 6: Variability of annual mean wave direction (Δθ, solid line) and cumulative annual energy ($\tau=H^2T$, dot line), between 1970 and 2008.

a) b)

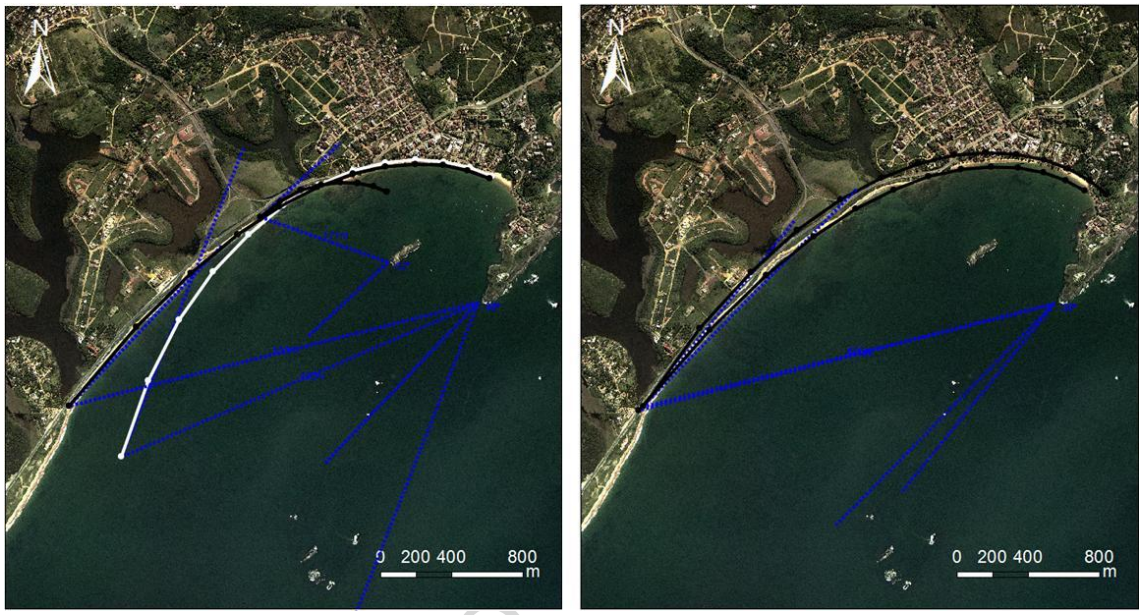

Figure 7: Northern Meaípe-Maimbá Beach (a) Planform modeled with waves adjusted to the coast in static equilibrium (black) and to the representative wave (white), (b) potential mobility as a function of seasonal variation in the direction of incident waves, where the innermost shoreline is associated with -4º change (NE) and the outermost shoreline with +4º change (SE).

a) b)

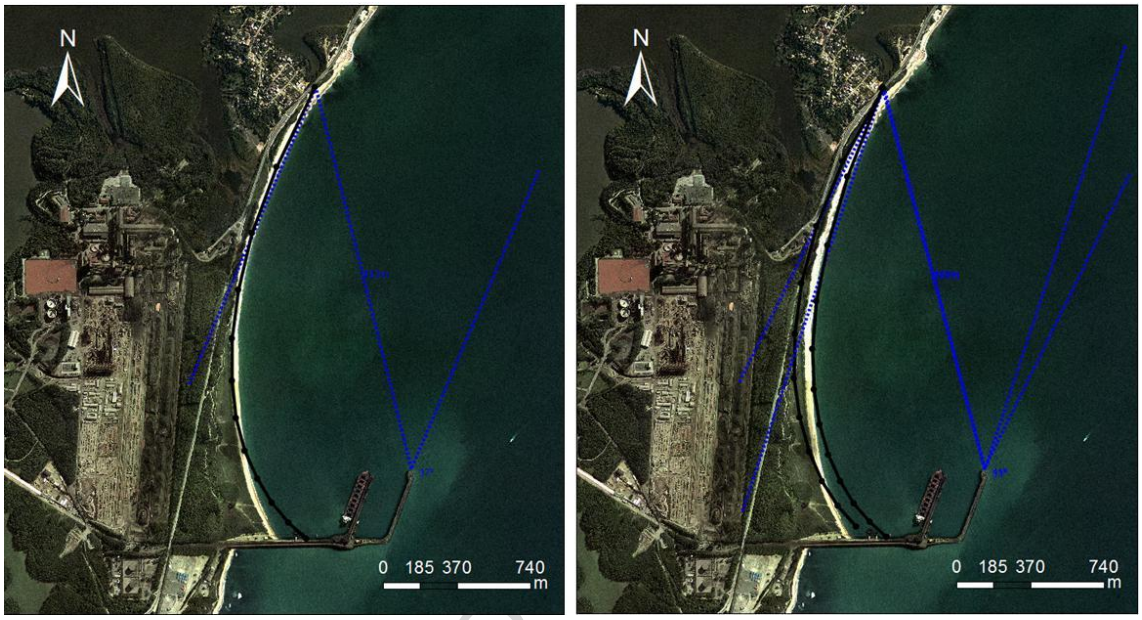

Figure 8: Meaípe-Maimbá South Beach (a) Planform in static equilibrium, (b) potential mobility in plan in terms of wave direction fluctuations. Inner line, increment of (+4°) SE waves.

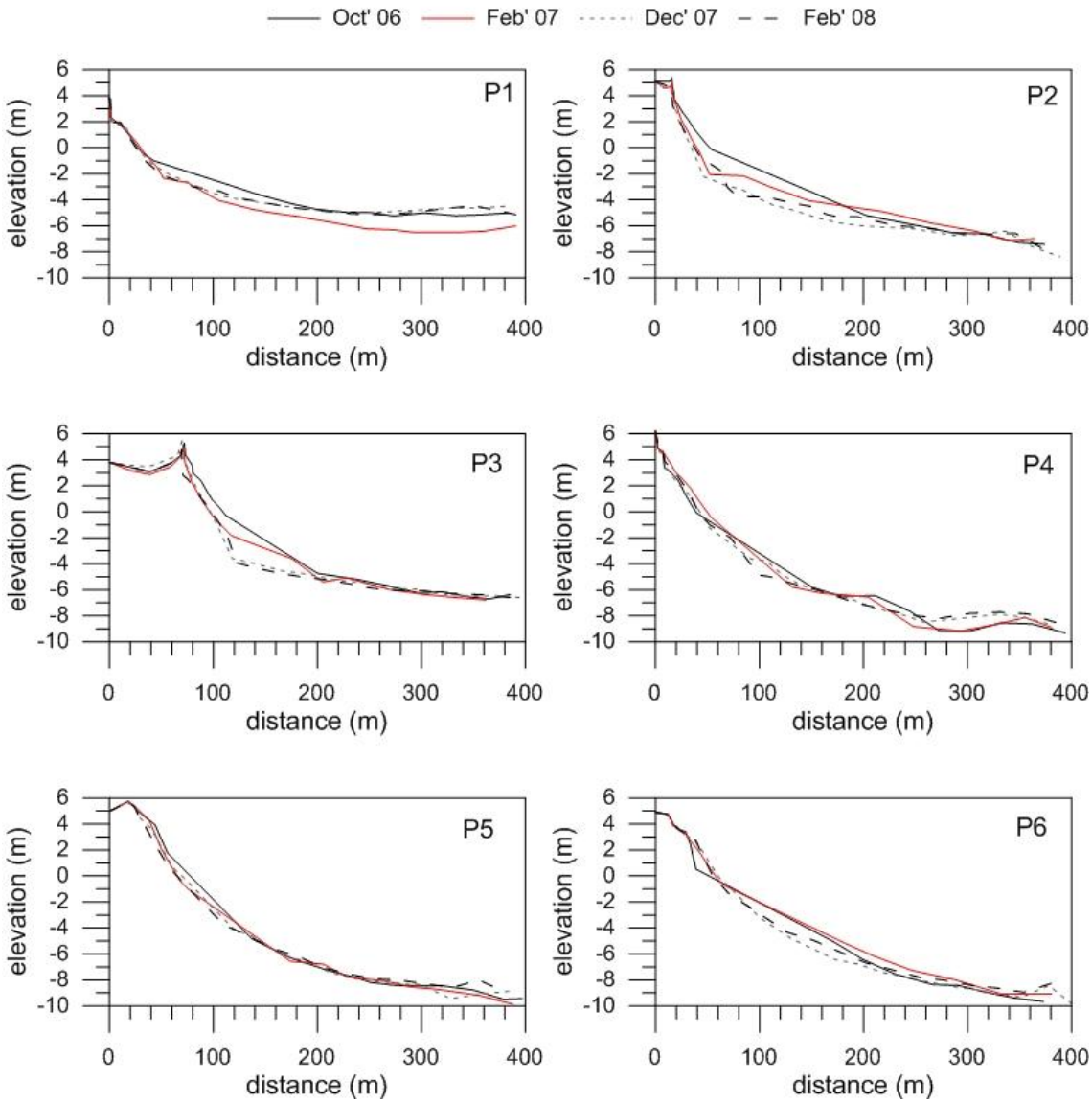

Figure 9: Morphological variation of the transversal profiles.

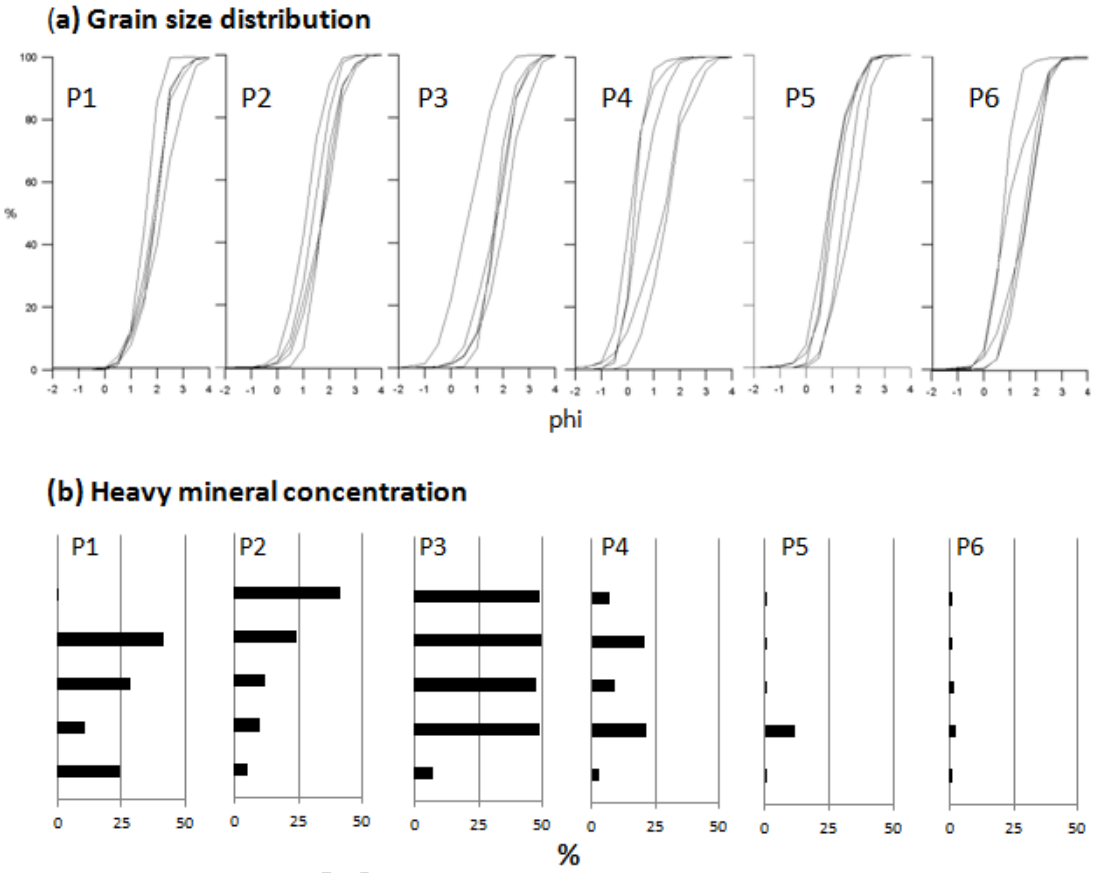

Figure 10: Grain size distribution and heavy mineral concentration.

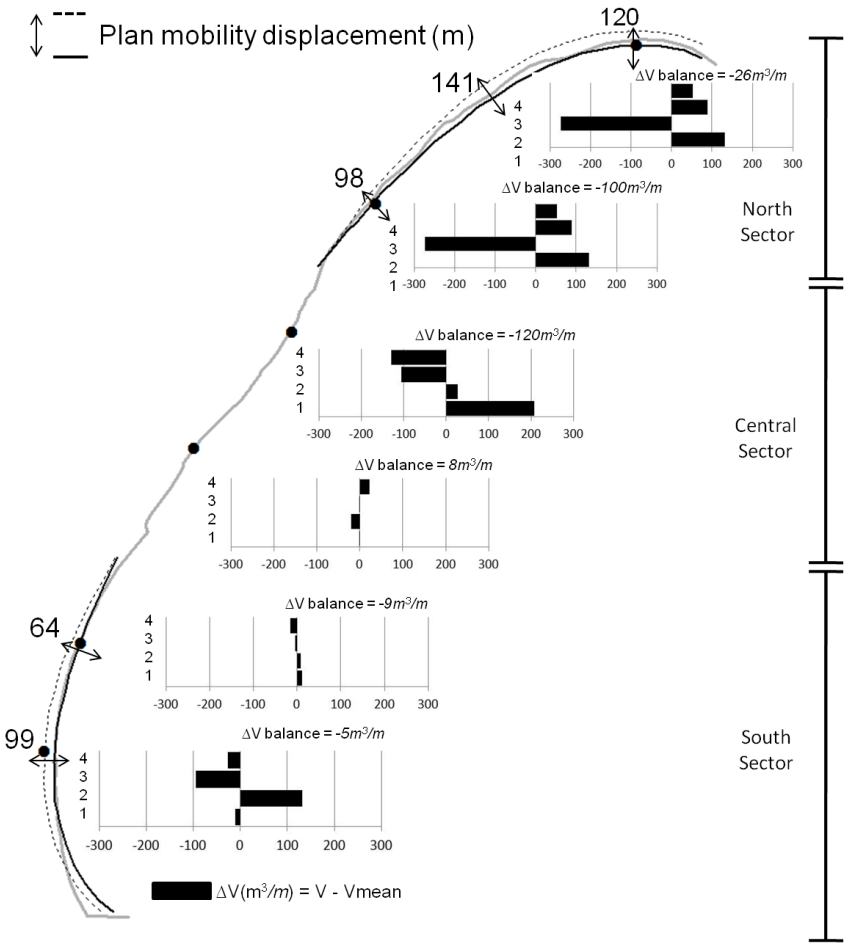

Figure 11: Planform and profile mobility. Profile Mobility is represented by the change in volume profiles (ΔV) of October 06 (1), February 07 (2), December 07 (3) and February 08 (4). Modeled plan mobility is identified by shorelines displacements (plan mobility displacement) induced by changes in wave direction (+/- 4°). Solid line, progradation and dotted line, retreat.

Table 1 - Mean error statistics for the hindcast data of significant wave height (H_s), peak wave period (T_p) and Mean Wave Direction (θ).

time		H_s (m)		T_p (s)		θ (°)	
Begin	End	Bias	RMSE	Bias	RMSE	Bias	RMSE
1/28/07	4/4/07	0.03	0.16	-0.33	1.93	12.95	41.52
9/29/07	10/25/07	0.02	0.17	0.02	1.55	7.51	19.38
11/23/07	12/18/07	-0.02	0.23	0.09	1.34	12.79	26.12
1/23/08	3/06/08	0.14	0.24	0.22	1.03	13.44	28.60

Table 2 Longhore sediment transport along the Meaípe-Maimbá beach, in 2008.

K (Value)	Q to the North (m^3/year)	Q to the South (m^3/year)	Net Q (m^3/year)
0.05-0.14	23 431	420 115	396 754

Table 3 - Fitting parameters that solve the parabolic bay model in the Meaípe-Maimbá Beach.

Arch	Diffraction point	Wave condition	R_0 (m)	C_0	C_1	C_2
North	Main headland	Geomorphological	2351	0.00329	1.20785	0.24080
	Inner island	Geomorphological	739	0.44963	2.33988	0.89025
South	Head of the breakwater	Representative	1873	0.01579	1.27835	-0.29413

Table 4 Mean values of profile morphological parameters.

	P1	P2	P3	P4	P5	P6
Width (m)	23.56	24.69	26.68	29.33	38.36	37.84
Berm Crest (m)	1.44	2.88	2.65	2.32	4.10	3.29
Beach slope (tan)	0.11	0.13	0.12	0.13	0.17	0.16

Table 5 Representative direction (θm) and accumulated energy (τm) of 30 days prior to survey. Representative direction and monthly accumulated energy in the survey year (θyear; τ/12).

	θm (°N)	τm (Kw/m)	θyear (°N)	τ/12 (Kw/m)
Oct 06	106.5	6.41	114	5.66
Feb 07	111.0	3.36	110	5.45
Dec 07	96.0	4.05	110	5.45
Feb 08	109.0	3.70	114	6.67

Table 6 - Mean values of sedimentological parameters based on 5 fields campaigns (Oct 06, Feb 07, Apr 07, Dec 07 and Feb 08)

	P1	P2	P3	P4	P5	P6
Sand mineralogy (%)						
Siliciclastic	78.16	81.00	59.17	87.14	96.60	98.51
$CaC0_3$	0.78	0.49	0.49	0.48	0.68	0.46
Heavy mineral	21.06	18.51	40.34	12.38	2.72	1.03
Grain size classification (phi)						
Median diameter (D_{50})	1.91 medium sand	1.56 medium sand	1.50 medium sand	1.45 medium sand	1.21 medium sand	1.29 medium sand
Standard deviation	0.66 moderately to well sorted	0.96 moderately sorted	0.82 moderately sorted	0.80 moderately sorted	0.66 moderately to well sorted	0.68 moderately to well sorted
Skewness	-0.13 negative assymmetry	-0.04 symmetry	0.04 symmetry	0.00 symmetry	0.06 symmetry	0.00 symmetry

Highlights

- The planform of an under-reported tropical embayed beach is studied.
- The parabolic bay model is applied to understand planform mobility processes.
- Annual and decadal beach mobility are discussed.
- Sedimentological and morphological field data are used to validate model results.